Nuclear Inst. and Methods in Physics Research B 450 (2019) 13–18
https://doi.org/10.1016/j.nimb.2018.05.018
Received 30 October 2017; Received in revised form 24 April 2018; Accepted 11 May;
2018 Available online 29 May 2018; Published 1 July 2019

Experimental determination of the $^{16}O(^3He,p_0)^{18}F$ differential cross section

Maria Guitart Corominas, Thomas Schwarz-Selinger
Max-Plank-Institut für Plasmaphysik, 85748 Garching, Germany

Abstract

The differential cross section for the $^{16}O(^3He,p_0)^{18}F$ nuclear reaction is measured for a reaction angle of 135° in the laboratory frame for ^3He energies between 1800 keV and 6100 keV. SiO_2 thin films thermally grown on crystalline Si were used as reference samples. Their oxygen content was quantified by ^3He Rutherford backscattering. The p_0 cross section shows several resonances with the largest reaching 6.2 mbarn/sr at 4400 keV. At 2390 keV the measured cross section value coincides nicely with the measurement of Lennard et al. [1]. As an example, the oxygen areal density of the native oxygen coverage of polycrystalline tungsten was determined to be $(11 \pm 1) \times 10^{15}$ O/cm^2.

1. Introduction

Surface coverage of metals with oxygen plays a crucial role in many fields of research and technology and its quantification is essential to understand the processes involved. The most popular way to quantify oxygen is the $^{16}O(\alpha,\alpha)^{16}O$ resonance at 3037 keV [2] with a cross section that exceeds the Rutherford cross section by nearly a factor of seven. However, for heavy

substrates like tungsten, even this enhanced cross section does not allow to determine trace amounts of ^{16}O, as the measured signal is dominated by the backscattering from the high Z substrate. Because the commonly proposed nuclear reaction ^{16}O(d,p$_1$)^{17}O is not possible in many IBA laboratories for regulatory reasons, Heggie et al. [3] proposed the ^{16}O(^{3}He,pγ)^{18}F nuclear reaction and provided the summed cross section for the production of three γ rays for ^{3}He energies between 2.6 and 4.0 MeV. Lennard et al. [1] determined for this reaction the absolute differential cross section for p$_0$ to p$_6$ under several reaction angles for a single ^{3}He energy of 2390 keV. Here we present absolute differential cross section measurements for the ^{16}O(^{3}He,p$_0$)^{18}F reaction at a reaction angle of 135° for ^{3}He energies in the laboratory frame between 1800 and 6100 keV. As an example for high Z materials, the oxygen areal density of the native oxide of polycristalline tungsten and deliberately oxidized tungsten is quantified.

2. Experiment

Experiments were conducted at the 30° beam line of the 3 MV tandetron accelerator at IPP Garching in the so-called rks analysis station. With the same setup, recently the differential cross sections for the D(^{3}He,p)^{4}He nuclear reaction were remeasured for different reaction angles [4].

To facilitate accurate current measurements the sample is surrounded by two concentric cylinders acting as Faraday shields. While the outer cylinder is grounded, the inner cylinder is biased to -120 V with respect to the target holder to repel secondary electrons. Openings in the cylinder, 5 and 6 mm in diameter, allow the beam to pass through and hit the sample. The beam size

is defined by a pair of orthogonal adjustable slits in front of these cylinders and is set to 1 x 1 mm^2 for these measurements. The current to both, the inner cylinder and the target holder is measured together and referred to as target current. Measurements are conducted with a preset charge rather than a constant time.

A Passivated Implanted Planar Silicon (PIPS) detector is positioned at 165° in Cornell geometry to measure backscattered primary ions (referred to as RBS detector). It has an aperture slit of 5 x 1 mm^2 and is 64.1 mm away from the target surface. The energy calibration as well as the detector solid angle were determined with 1.0 MeV and 1.5 MeV ^{4}He using bulk spectra of Au, Rh, Co, and Al, and simulating the spectra with SIMNRA 6.06 [5] applying SRIM-2003 stopping powers [6]. The measured solid angle based on these bulk spectra is (1.108 ± 0.038) msr. It coincides with calibrations performed with IRMM targets [7] within the error bar of the measurements. The depletion depth for this detector is measured to be about 500 μm. In addition to the measurement of current collected at the target holder this detector facilitates hence absolute measurements of the incoming number of particles by evaluating the backscatter signal.

The high energetic protons from the nuclear reaction are collected simultaneously with a second PIPS detector, referred to as proton detector in the following. It is placed under a reaction angle of 135° in IBM geometry to the incoming beam. It is located 41 mm away from the sample surface and has a parabolic slit with a width of 3 mm to reduce the scattering angle to ± 2°. The solid angle was determined from ^{3}He measurements with a 270 nm thick amorphous deuterated carbon thin films on silicon at a primary ^{3}He energy

of 800 keV. For this energy the D(^{3}He,p)^{4}He cross section can be considered isotropic. Therefore the ratio of the peak integrals of the proton peak visible in both detectors - the RBS and the proton detector - reflects the ratio of the solid angles of the two detectors. With the known solid angle for the RBS detector from above the solid angle of the proton detector was determined to be 30.26 $\pm$ 1.18 msr. The Q-value for the present nuclear reaction is 2031.8 keV and hence, a detector thickness of 400 μm is enough to fully stop the protons. As the setup is designed to fully stop the 12 MeV protons from the D(^{3}He,p)^{4}He, the detector has a depletion depth of 2000 μm. A 5 μm thick Ni foil and a 12 μm-thick Mylar foil, coated with 100 Å Au, is placed in front of the detector to stop backscattered ^{3}He. The energy calibration was performed by measuring a 270 nm thick amorphous deuterated carbon thin film on silicon at a primary ^{3}He energy of 2400 keV parameters. Narrow resonances of the p_0, p_1, and p_2 protons from the ^{12}C(^{3}He,p)^{14}N together with the protons from the D(^{3}He,p)^{4}He reaction allow accurate energy calibration between 1.5 and 12.3 MeV.

The accelerator terminal voltage was calibrated for protons with the ^{27}Al(p,γ)^{28}Si resonances at 992 and 1380 keV. The beam energy spread was found to be below 0.1% for protons at 1000 keV. A calibration for ^{4}He ions was performed with the ^{16}O(α,α)^{16}O resonances at 3036 and 3877 keV. Peak positions were within $0.4 - 0.5\%$.

3. Results

3.1. SiO_2 reference samples

As reference samples for the cross section measurements thermally grown SiO_2 thin films on Si $\langle 001 \rangle$ were used. Two different thickness were chosen for the analysis. A thick film was used for good counting statistics (called "thick SiO_2" in the following) while a nine times thinner one was used (called "thin SiO_2" in the following) to minimize energy loss and energy straggling in the film for the later cross section measurements.

The absolute oxygen content was determined quantitatively for both by Rutherford backscattering.

Figure 1 shows the signal of the backscattered spectrum for a primary ^{3}He ion beam energy of 2150 keV for the "thick SiO_2". A charge of 20 μC was acquired on a beam spot of 1x1 mm^2. The oxygen content can be derived from the height of the Si backscattered signal between 1380 keV and 1015 keV as well as from the width of the oxygen peak between 1000 keV and 615 keV. Also visible in figure 1, is the backscatter peak from a 100 Å thin Au top layer at 2000 keV. This metal coating improves surface conductivity and, as will be outlined below, its backscatter signal was used to improve the accuracy of the current measurement. Also shown in figure 1, is the simulation calculated with MultiSIMNRA [8] that coincides with the measurement nicely. This fit was derived using the spectrum at the displayed energy (2150 keV) together with a RBS spectrum measured at 2400 keV primary ^{3}He energy. Besides the absolute areal density and the layer composition, the offset and the gain of the energy calibration, the product of the solid angle times the number of collected ions, and the layer roughness were fitted. SRIM 2008

stopping powers were used. An areal density of (3670 ± 10) × 10^{15} O/cm^2 and (1970 ± 5) × 10^{15} Si/cm^2 was the result for the thick SiO_2. The analysis for the thin SiO_2 layer was (410 ± 5) × 10^{15} O/cm^2 and (229 ± 5) ×10^{15} Si/cm^2, showing that both films were stoichiometric SiO_2.

3.2. Proton integrals

Figure 2 shows the proton spectra for three different incident ^{3}He energies as measured for the thick SiO_2 with the proton detector. For 2400 keV several peaks are visible in the spectrum that can be attributed to the protons p_0 to p_6 as shown in fig. 2a). Except for the p_0 peak, all of them overlap and individual contributions are not easily discernible. Therefore, only p_0 was chosen here for the evaluation in the following. It neither overlaps nor shows any significant background at this energy.

With increasing energy however, a clear background evolves. Apart from the protons resulting from reactions related to oxygen, protons created by nuclear reactions with other elements obviously reach the detector. To access the protons resulting from the nuclear reactions with silicon ^{28}Si(^{3}He,$p_{0,1,2,3,4}$)^{30}P [9], a single crystal Si wafer from the same batch was measured at every energy and the spectra are also plotted in Fig. 2. To have identical conditions this reference wafer was also coated with a 100 Å thin Au top layer. To a lesser extent, protons from reactions with other impurities such as carbon, can also appear: ^{12}C(^{3}He,$p_{0,1,2}$)^{14}N and ^{13}C(^{3}He,$p_{0,1,2,3}$)^{15}N. Despite a base pressure of 10^{-9} mbar, the unavoidable presence of hydrocarbons in the vacuum chamber ensue a high energetic proton peak from this nuclear reaction, which was observed to grow with accumulated charge. However, the influence of these protons was irrelevant for the quantification

of the p_0 peak. As can be seen in Fig. 2, subtraction of the signal stemming from Si already allows for an accurate background subtraction.

3.3. Absolute Charge Measurement

The accuracy of the current measurement is known to be within ± 3% for the given setup. In order to reduce this even further, a roughly 100 Å thick Au layer ($\approx 64\times10^{15}$ Au/cm^2) was deposited onto the SiO_2 by means of vacuum evaporation. The backscatter signal of this Au layer in the RBS detector was integrated and compared with the theoretical value derived by SIMNRA as shown in Fig. 3. This allows to find possible outliers as well as reduce the scatter. Since the absolute Au amount as well as the error in the solid angle of the detector and the collected charge do not have to be taken into account, the error bar reduces to the counting statistics which equates to 0.5 % at 1800 keV and 1.5 % at 6000 keV for the given measurement. It is worth mentioning that while at the maximum energy ^{3}He scattering on Au follows the Rutherford cross section, a slight modification needs to be considered at lower energies, due to electron screening effects. This deviation is quantified by the Andersen factor [10] and implies a reduction in the cross section of up to 1.12 % at 1800 keV. The ratio of the measured integral and the calculated value gives the correction factor for each energy and it is then used to scale the proton integrals to account for the correct charge acquired.

3.4. Absolute differential cross section

The background subtracted peak integral of the p_0 proton spectrum, i.e. the number of detected particles, is proportional to the differential cross section σ. The proportionality factor is given by equation 1, where r is the

number of protons (see section 3.2), Φ is the product of the detector's solid angle times the number of collected ^{3}He ions (see 2 and 3.3), and ρ is the areal density of oxygen atoms in the sample (see 3.1).

$$r = \Phi \cdot \rho \cdot \sigma \tag{1}$$

The result derived from both measurement series with the thick and the thin sample is shown in Fig. 4 as function of the corrected ^{3}He energy. The latter was derived by subtracting from the primary ^{3}He the total energy loss in the Au film and half the energy loss in the SiO_2, as calculated with SRIM stopping powers [6] with SIMNRA [5]. Depending on primary ^{3}He ion energy this results in energy losses between 213 and 97 keV, for the thick SiO_2, and between 27 and 13 keV, for the thin SiO_2. The energy loss in the Au film is only between 3.8 and 6.4 keV.

The given uncertainty of the individual data points is determined by the statistical uncertainty associated to both the sum of the proton peak and the Si background signal, the uncertainty in the solid angle of the detector, and the uncertainty in the areal density of the oxygen layer. The total uncertainty is the quadratic sum of all of individual error bars as they are independent from each other.

The thin SiO_2 film was measured in steps of 25 keV and the thick SiO_2 films in steps of 50 keV. As one can see in Fig. 4, both measurements give the same result within the error bars. No significant difference is observed in terms of the width of the high energetic resonances at 4500 and 5000 keV. Both samples can be considered thin layers and the energy spread or energy resolution is not influencing the peak width. In addition to the measurement

results, the value of Lennard [1] measured at 2390 keV ^{3}He energy and 133.9° is shown as green circle. It coincides nicely with the present measurements and shows that Lennard picked the first resonance at these low energies. However, as can be seen from Fig. 4 it is advisable to measure at larger energy as the resonances at 4000 and 5000 keV have a cross section that is with 6.3 mbarn more than four times larger.

With these two energies the oxygen areal density of the native oxygen coverage of a polycrystalline tungsten sample was determined to be (11 ± 1) $\times 10^{15}$ O/cm^2. A charge of 20 μC was acquired on a beam spot of 1x1 mm^2 to achieve an acceptable counting statistic. In contrast to the Si substrate for tungsten, there is no background signal that interferes with the p_0 peak. To make sure that this is the case, a tungsten sample was deliberately oxidized in oxygen atmosphere at 400°C. For this heavily oxidized sample the oxygen content can even be inferred from the step height in the RBS spectrum to be (1650 ± 60) $\times 10^{15}$ O/cm^2. From the p_0 intensity at 4450 keV and 3100 keV primary ^{3}He energy a value of (1570 ± 100) $\times 10^{15}$ O/cm^2) is inferred, which proofs the applicability of the method for tungsten.

4. Conclusions

In this work, the differential cross section for ^{16}O(^{3}He,p)^{18}F has been experimentally determined in an energy range from 1800 keV to 6100 keV for a scattering angle of 135°. The value of the cross section at 2390 keV given by Lennard *et al.* [1] coincides with the measurements, and the shape of the cross section agrees with the study done by J.C.P Heggie *et al.* [3] measured by means of the de-exciting γ rays. For energies above 5000 keV, the cross

section measurement is less reliable due to a large background signal, as a result of reactions of incoming ^{3}He with the silicon present in the sample.

Acknowledgments

We thank Stefan Kapser to draw our attention to this topic and Matej Mayer for his support. The MultiSIMNRA fit of the RBS spectra by Tiago Silva is greatly appreciated. Help of Joachim Dorner and Michael Fusseder for operating the tandem and of Karsten Schlüter for preparing the thin SiO_2 film is greatly acknowledged.

Bibiography

[1] W.N. Lennard, S.Y. Tong, I.V. Mitchell, G.R. Massoumi, Nucl. Instr. & Meth. **B43** (1989) 187-192

[2] IBANDL IAEA data base: https://www-nds.iaea.org/exfor/ibandl.htm

[3] J.C.P. Heggie, Z.E. Switkowski, G.J. Clark, Nucl. Instr. & Meth. **168** (1980) 125-129

[4] B. Wielunska, M. Mayer, T. Schwarz-Selinger, U. von Toussaint, J. Bauer, Nucl. Instr. & Meth. **B371** (2016) 41-45

[5] M. Mayer (http://home.mpcdf.mpg.de/ mam/)

[6] J.F. Ziegler, www.srim.org

[7] Reference Laboratory for Neutron Measurements of the IRMM, Geels, Belgium

[8] T.F. Silva, C.L. Rodrigues, M. Mayer, M.V. Moro, G.F. Trindade, F.R. Aguirre, N. Added, M.A. Rizzutto, M.H. Tabacniks, Nucl. Instr. Meth. **B371** (2016) 86-89

[9] K.O. Groeneveld, B. Hubert, R. Bass, H. Nann, Nucl. Phys. **A151** (1970) 198-210

[10] H.H. Andersen, F. Besenbacher, P. Loftager, W. Moeller, Phys. Rev. **A21.6** (1980) 1891-1901

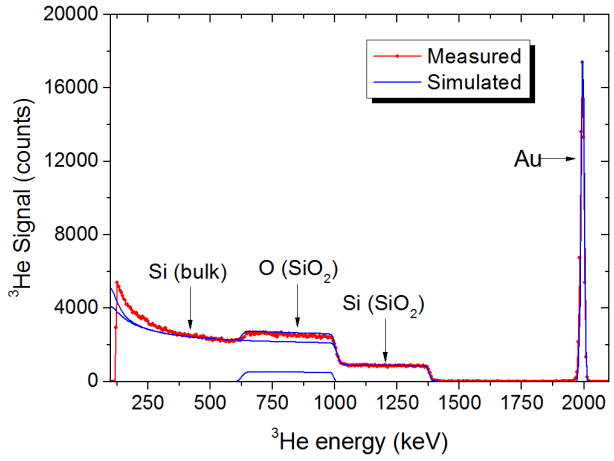

Figure 1: RBS spectrum of 2150 keV ^{3}He backscattered from the "thick SiO_2" sample (red symbols) and the MultiSIMNRA fit (blue line) showing the Si edge at the surface, the reduced Si step height as well as the O peak of the SiO_2 film. In addition the peak of the Au top layer is observed. 20 μC were acquired on a beam spot of 1x1 mm^2.

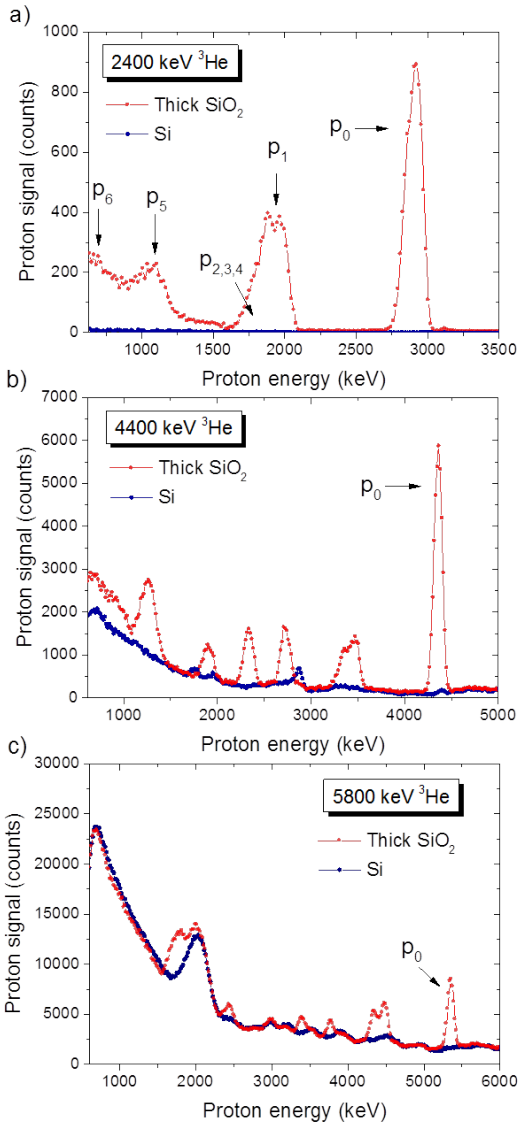

Figure 2: Proton energy spectra for ^{3}He incident energies of a) 2400 keV, b) 4400 keV and c) 5800 keV for the thick SiO_2 layer (red symbols) and the Si reference (blue symbols). With increasing energy protons stemming from a nuclear reaction with Si lead to a substantial background signal.

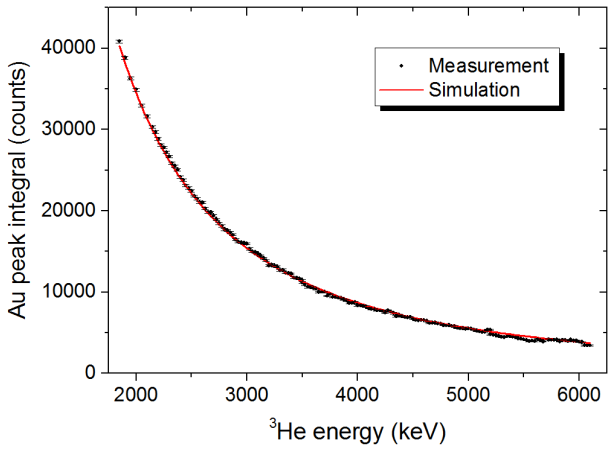

Figure 3: Au peak integral as function of primary ^{3}He energy (black symbols) for the thin SiO_2 in steps of 25 keV together with the error bars derived from counting statistics. A nominal charge of 10 μC was acquired for each data point. The simulation was derived with SIMNRA [5] with screening effects described by Andersen [10].

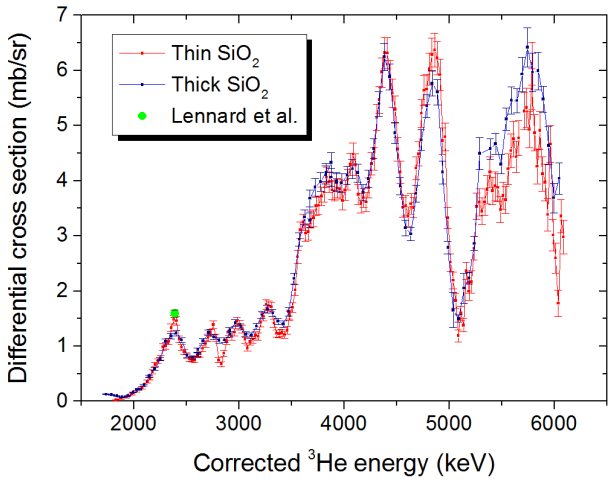

Figure 4: Absolute differential cross section for the ^{16}O(^{3}He,p)^{18}F reaction, for a reaction angle of 135° measured with the thin SiO_2 film in 25 keV steps and with the thick SiO_2 films in 50 keV steps. In addition the value of Lennard [1] measured at 133.9° is shown as green circle.

Energy (keV)	**Cross section (mb/sr)**	**Total uncertainty in percentage**
1830.0	0.021	28
1880.2	0.050	18
1930.5	0.72	15
1980.7	0.13	11
2030.9	0.19	9.5
2081.2	0.24	8.6
2131.4	0.36	7.5
2156.5	0.41	7.1
2181.6	0.55	6.5
2206.7	0.66	6.1
2231.8	0.73	5.9
2256.9	0.79	5.8
2282.0	0.98	5.5
2307.1	1.0	5.5
2332.2	1.1	5.4
2357.3	1.3	5.2
2382.4	1.5	5.1
2407.5	1.5	5.1
2432.6	1.1	5.4
2457.7	0.98	5.5
2482.8	0.90	5.7
2507.9	0.83	5.8
2533.0	0.77	5.9

2558.1	0.76	6.0
2583.1	0.75	6.0
2608.2	0.84	5.8
2633.3	0.86	5.8
2658.4	0.95	5.6
2683.5	1.0	5.5
2708.6	1.2	5.4
2733.6	1.2	5.3
2758.7	1.4	5.2
2783.8	1.2	5.4
2808.9	0.75	6.2
2834.0	0.68	6.3
2859.0	0.87	5.8
2884.1	1.1	5.5
2909.2	1.3	5.3
2934.3	1.2	5.4
2959.3	1.3	5.4
2984.4	1.4	5.2
3009.5	1.4	5.2
3034.5	1.3	5.3
3059.6	1.1	5.5
3084.7	1.0	5.8
3109.7	1.1	5.6
3134.8	1.1	5.5

3159.9	1.2	5.5
3184.9	1.2	5.4
3210.0	1.4	5.2
3235.1	1.5	5.2
3260.1	1.8	5.0
3285.2	1.7	5.0
3310.3	1.7	5.1
3335.3	1.4	5.3
3360.4	1.2	5.5
3385.4	1.2	5.5
3410.5	1.2	5.4
3435.6	1.2	5.6
3460.6	1.3	5.5
3485.7	1.6	5.2
3485.7	1.6	5.2
3510.7	1.7	5.1
3535.8	2.0	4.9
3560.9	2.6	4.8
3585.9	3.1	4.6
3611.0	3.2	4.6
3636.0	3.0	4.7
3661.1	3.1	4.7
3686.1	3.3	4.6
3711.2	3.3	4.6

3736.2	3.5	4.6
3761.3	3.6	4.6
3786.3	3.7	4.6
3811.4	3.8	4.6
3836.4	4.1	4.5
3861.5	4.0	4.6
3886.5	3.8	4.6
3911.6	3.8	4.6
3936.6	3.9	4.6
3961.7	3.9	4.6
3986.7	3.6	4.7
4011.8	3.8	4.7
4036.8	4.0	4.7
4061.9	4.3	4.6
4086.9	4.5	4.6
4112.0	4.3	4.6
4137.0	3.7	4.7
4162.1	3.6	4.8
4187.1	3.7	4.7
4212.2	3.6	4.8
4237.2	3.9	4.7
4262.2	4.3	4.7
4287.3	4.4	4.7
4312.3	5.1	4.6

4337.4	5.5	4.5
4362.4	6.0	4.5
4387.5	6.3	4.5
4412.5	6.3	4.5
4437.5	5.9	4.5
4462.6	5.6	4.6
4487.6	5.3	4.6
4512.7	4.6	4.7
4537.7	4.2	4.8
4562.7	3.5	5.2
4587.8	3.5	5.2
4612.8	3.3	5.3
4637.9	3.6	5.2
4662.9	3.5	5.3
4687.9	4.2	5.0
4713.0	4.5	4.9
4738.0	5.2	4.9
4763.1	5.6	4.8
4788.1	5.7	4.9
4813.1	6.0	4.8
4838.2	6.3	4.8
4863.2	6.4	4.8
4888.2	6.2	4.8
4913.3	5.9	4.8

4938.3	4.7	5.1
4963.3	4.8	5.2
4988.4	3.3	5.7
5013.4	2.5	6.3
5038.5	2.2	7.0
5063.5	1.8	7.4
5088.5	1.2	9.1
5113.6	1.6	8.1
5138.6	1.4	8.7
5163.6	2.4	6.6
5188.7	2.0	8.0
5188.7	2.2	8.9
5213.7	2.2	9.3
5238.7	2.8	7.6
5263.8	3.5	6.8
5288.8	3.6	6.7
5313.8	3.4	7.0
5338.9	3.6	6.6
5363.9	3.8	6.6
5388.9	4.2	6.7
5414.0	3.8	6.4
5439.0	3.9	6.7
5464.0	3.9	6.6
5489.0	3.5	6.9

5514.1	3.7	6.6
5539.1	3.7	6.9
5564.1	4.2	6.6
5589.2	4.5	6.7
5614.2	4.8	6.8
5639.2	4.4	6.4
5664.3	4.8	6.6
5714.3	5.3	6.4
5739.3	5.3	6.7
5764.4	4.9	6.6
5789.4	6.1	6.3
5789.4	5.7	6.5
5814.4	4.9	6.7
5839.5	4.3	7.5
5864.5	4.9	7.0
5889.5	4.1	7.6
5914.5	4.0	8.4
5939.6	3.4	8.7
5964.6	4.7	7.1
5989.6	3.0	9.5
6014.6	2.6	10
6039.7	1.8	13
6064.7	3.4	9
6089.7	3.0	10

Table 1: Absolute differential cross section as a function of corrected energy for $^{16}O(^{3}He,p_0)^{18}F$, measured with "thin SiO_2"

Energy (keV)	**Cross section (mb/sr)**	**Total uncertainty in percentage**
1738.8	0.13	5.2
1790.4	0.12	5.3
1842.0	0.095	5.6
1893.5	0.077	5.9
1944.9	0.098	5.5
1996.4	0.16	5.0
2047.8	0.22	4.7
2047.8	0.22	4.6
2099.1	0.30	4.4
2150.4	0.46	4.3
2201.7	0.59	4.2
2252.9	0.77	4.1
2304.1	1.1	4.1
2355.3	1.2	4.1
2406.4	1.2	4.1
2457.5	1.1	4.1
2508.6	0.83	4.1
2559.7	0.79	4.1

2610.7	0.85	4.1
2610.7	0.93	4.1
2661.7	1.1	4.1
2712.6	1.2	4.1
2763.6	1.2	4.1
2814.5	1.1	4.1
2865.4	1.1	4.1
2916.3	1.2	4.1
2916.3	1.3	4.1
2967.2	1.4	4.1
3018.0	1.4	4.1
3068.8	1.2	4.1
3119.6	1.2	4.1
3170.4	1.4	4.1
3221.2	1.6	4.1
3271.9	1.7	4.0
3322.6	1.6	4.0
3373.4	1.4	4.0
3424.1	1.4	4.2
3474.7	1.6	4.6
3525.4	2.2	4.3
3576.1	2.9	4.0
3626.7	3.3	4.0
3677.3	3.3	4.0

3677.3	3.7	4.1
3728.0	3.9	4.1
3778.6	4.0	4.1
3829.2	4.1	4.0
3829.2	4.1	4.0
3879.8	4.3	4.1
3879.8	4.1	4.2
3930.3	4.0	4.1
3930.3	4.0	4.2
3980.9	4.0	4.2
4031.4	4.1	4.0
4082.0	4.2	4.2
4132.5	4.1	4.0
4183.0	3.8	4.0
4233.6	4.0	4.0
4284.1	4.6	4.0
4334.6	5.4	4.1
4385.0	6.2	4.0
4435.5	5.9	3.9
4486.0	4.9	4.0
4536.5	3.9	4.0
4586.9	3.1	4.4
4637.4	3.0	4.0
4687.8	3.8	4.1

4738.2	4.7	4.0
4788.7	5.4	4.0
4839.1	5.8	4.0
4889.5	5.6	4.1
4939.9	4.2	5.0
4990.3	2.8	4.1
5040.7	1.7	19.2
5091.1	1.5	4.6
5141.5	2.0	13.5
5191.9	2.2	4.7
5242.2	2.9	4.4
5292.6	4.5	6.5
5393.3	4.6	4.1
5443.7	4.7	4.0
5494.0	4.3	4.1
5544.4	5.1	4.0
5594.7	5.5	4.4
5645.0	5.5	4.1
5695.4	5.9	5.3
5745.7	6.4	5.5
5796.0	6.0	5.8
5846.3	6.0	5.6
5896.6	5.5	4.3
5947.0	4.6	7.4

5997.3	3.7	7.2
6047.6	4.0	7.0

Table 2: Absolute differential cross section as a function of corrected energy for $^{16}O(^{3}He,p_0)^{18}F$, measured with "thick SiO_2"